

Enamel fluorosis in rat's incisor: S.E.M. and T.E.M. investigation

S. PERGOLIZZI, Ant. SANTORO, G. SANTORO, F. TRIMARCHI, G. ANASTASI

Department of Biomorphology, University of Messina

SUMMARY

Findings on the alterations taking place in the enamel have demonstrated that they are generally caused by a daily use of highly fluoritic drinking waters.

According to that, the Authors have carried out an ultrastructural study on lower incisors of albino rats after administering for 60 days water with a fluorine concentration five times the normal one.

The samples, studied under the S.E.M., showed a general slowing of both the deposition and the maturation phase as well as the presence of some hypomineralized areas even after eruption.

All this suggested the possibility that the damages observed were not due to the direct effect of fluorine on the enamel, but to the interaction between fluorine and ameloblasts.

The Authors have then carried out an ultrastructural study on the enamel organ using the S.E.M.

The results showed the presence of a well-evident endoplasmic reticulum, the lack in dense granules during the secretion phase, the lack in ruffle ended webs during the modulation phase, and the mitochondrial damage in the ameloblast.

All this could justify the slowing of the enamel mineralization caused by fluorine effect on the ameloblasts.

KEY WORDS:

Enamel - Rod - Interrod - Ameloblast - Fluorosis

RÉSUMÉ

Il a été démontré que des altérations de l'émail sont généralement dues à l'absorption quotidienne d'eaux de boissons riches en fluor.

Les auteurs ont entrepris une étude ultrastructurale des incisives inférieures du rat ayant reçu pendant 60 jours de l'eau dont la concentration en fluor est 5 fois supérieure à la normale.

Les échantillons étudiés en microscopie électronique à balayage ont montré un ralentissement global de la déposition et de la phase de maturation ainsi que la présence de territoires hypominéralisés même après l'éruption.

Toutes ces constatations suggèrent la possibilité que les dommages observés ne sont pas dus à l'effet direct du fluor sur l'émail, mais aux interactions entre le fluor et les améloblastes.

Les auteurs ont mené une étude ultrastructurale de l'émail en utilisant le microscope électronique à balayage.

Les résultats ont montré la présence d'un réticulum endoplasmique bien apparent, l'absence de grains denses au cours de la phase sécrétoire, l'absence d'extrémités membranaires rugueuses au cours de la phase de modulation, et des altérations des mitochondries dans les améloblastes.

Toutes ces constatations pourraient expliquer le ralentissement de la minéralisation de l'émail causé par les effets du fluor sur les améloblastes.

MOTS CLÉS:

Email - Prisme - Interprisme - Améloblastes - Fluorose

INTRODUCTION

Previous studies on the enamel fluorosis showed a slowing of mineralization in the lower incisor of albino rats fed on hyperfluoritic pellet as well as a consequent hypomineralization in various zones of the enamel after eruption (Anastasi *et al.*, 1990).

Since the substitution of OH⁻ for fluorine causes a stabilizing effect on the enamel hydroxyapatite crystals (Eanes, 1979), we also assumed that the slowing of mineralization could be due to the interaction between fluorine and ameloblasts (Anastasi *et al.*, 1990; Magaudda *et al.*, 1990).

It has already been demonstrated that the fluorosis, characterized by a white to brown mottled enamel, is generally due either to a continuous use of fluoritic drinking water or to several rinsings with fluorine solutions (Kruger, 1966; La Spada and Busà, 1968; Sortino *et al.*, 1968; Leverett *et al.*, 1986).

According to what just said our first aim is to explore under the S.E.M. the possible effects of highly fluoritic water on the enamel and to compare them with those we already obtained administering hyperfluoritic pellet.

In order to do that, even this time we used the lower incisor of albino rats and we quintuplicated the maximum normal dose for two life cycles of ameloblasts.

The second aim of this study is to explore the possible interaction between fluorine and ameloblasts during the various stages of amelogenesis so that to correlate possible damages to the ameloblasts with the supposed alterations of enamel mineralization.

To this purpose we removed from each incisor the enamel organ and we examined it under the T.E.M.

MATERIALS AND METHODS

Sprague-Dowley rats with an average weight of 150 g were used. After one week of normal stalling the rats were fed for 60 days on usual pellet and fluoritic drinking water. The quantity of water drunk during

this period (two amelogenetic cycles) corresponded to the water drunk during the normal stalling.

The rats were killed after being chloroformed. Then the animals were perfused through the left ventricle using 4% glutaraldehyde in phosphate buffer 0,2 M (pH 7.2-7.4).

The lower incisors were then removed as well as their enamel organs. The incisors were studied under the S.E.M. while the enamel organs under the T.E.M.

S.E.M.

The lower incisors were fixed in 4% glutaraldehyde in phosphate buffer 0,2 M. After 24h and after rinsing them in phosphate buffer, the teeth were transversally fractured at 4/8/12/16 mm. from the cervical loop.

Immediately after the eruption, that is at about 24 mm. from the cervical loop, another fracture was carried out. The samples were first dehydrated in alcohol and dried at CO₂ critical point to be then sputtercoated with gold and observed under the S.E.M. Cambridge Stereoscan 200 at 20 KV.

T.E.M.

The enamel organs, after rinsing in phosphate buffer, were fixed in 1% osmium tetroxide in phosphate buffer 0,2 M (pH 7.2 - 7.4), dehydrated in alcohol and then embedded in Durcupan.

Semithin and ultrathin sections were cut: the semithin sections were stained with toluidine blue and observed under the L.M. Olympus BH2 while the ultrathin ones were stained with uranyl acetate and lead citrate Reynolds (1963) and observed under the T.E.M. Philips CM10.

RESULTS

Enamel

At the end of the deposition zone, that is at 6 mm. from the cervical loop, the two enamel prismatic layers are observable while the deposition of the outer aprismatic layer has not started yet.

In the innermost enamel prismatic layer, enamel subunits gather together to form the rods and the interrod (Fig. 1): the rod subunits are parallel to one another and to the mayor axis of the rod, while the interrod subunits are gradually divergent.

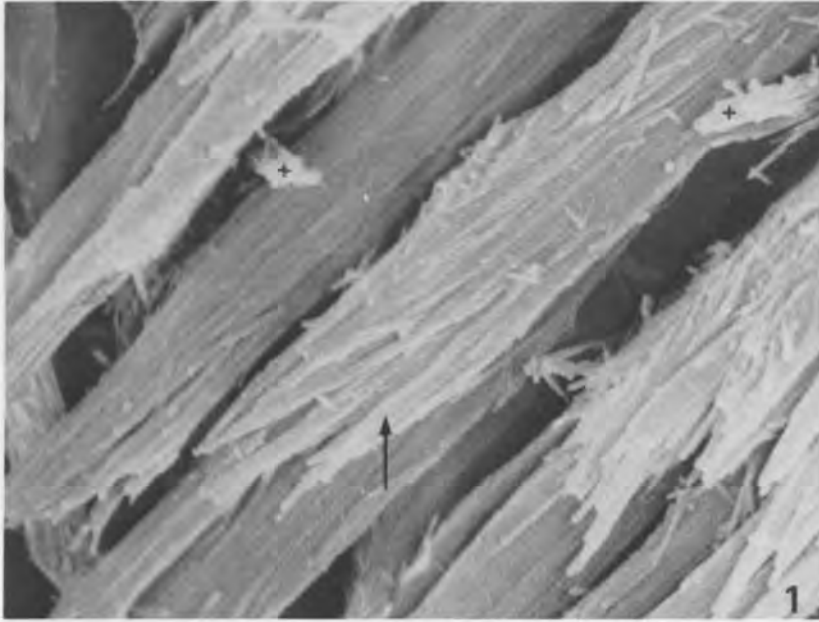


Fig. 1: 6 mm. from the cervical loop (end of the deposition zone): enamel subunits gather together to form the rods (\rightarrow) and the interrod (*). 13.000 \times .

Fig. 1: A 6 mm de l'anse cervicale (fin de la zone de dépôt): subunités d'émail les unes contre les autres formant des prismes (\rightarrow) et des interprismes (). 13.000 \times .*

Examining the outer enamel layer, because of the amorphous matrix in which the subunits are placed, their identification becomes step by step more difficult (Fig. 2).

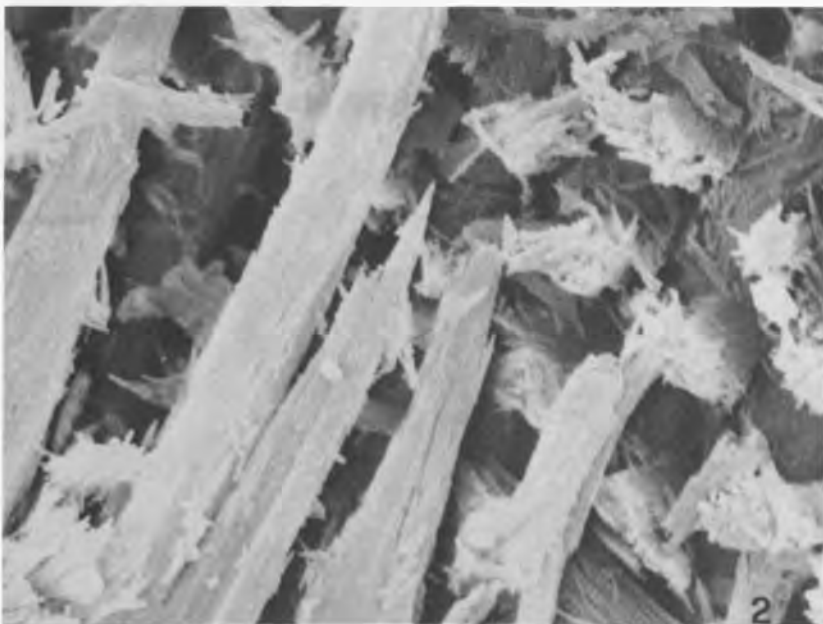


Fig. 2: 6 mm. from the cervical loop (end of the deposition zone): the identification of the subunits is difficult in the outer enamel layers. 8.000 \times .

Fig. 2: A 6 mm de l'anse cervicale (fin de la zone de dépôt): l'identification des sous-unités est difficile dans les couches d'émail plus superficielles. 8.000 \times .

Between the end of the deposition zone and the beginning of the maturation zone, that is at 8 mm. from the cervical loop, the rods are clearly identifiable (Fig. 3), but only in the innermost enamel layer.

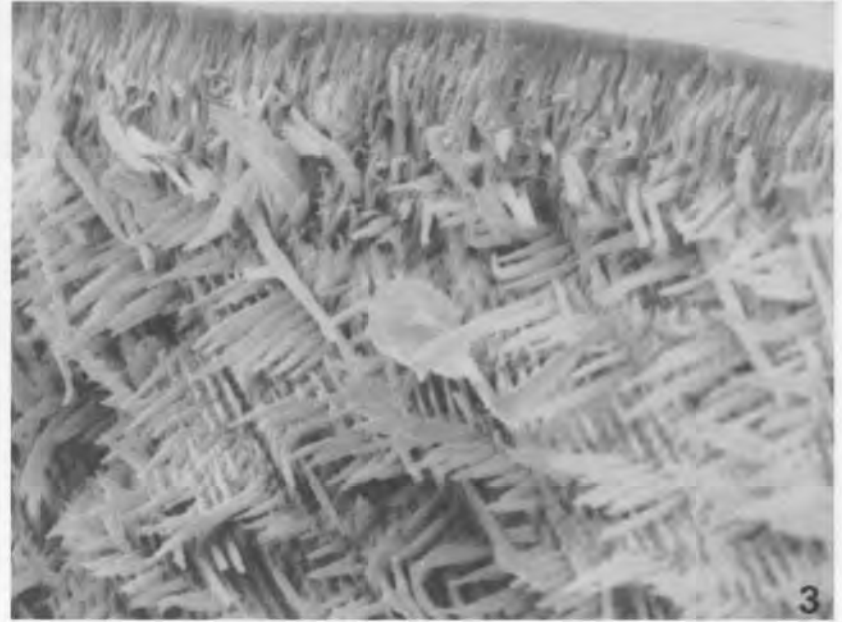


Fig. 3: 8 mm. from the cervical loop (end of the deposition zone – beginning of the maturation zone): the rods are clearly identifiable while no interprismatic enamel is observable. 1.100 \times .

Fig. 3: A 8 mm de l'anse cervicale (fin de la zone de dépôt – commencement de la zone de maturation): les prismes sont clairement identifiables alors qu'aucun émail interprismatique n'est observable. 1.100 \times .

Therefore, in this region some rods subunits are still observable (Fig. 4) while no interrod subunit is visible.

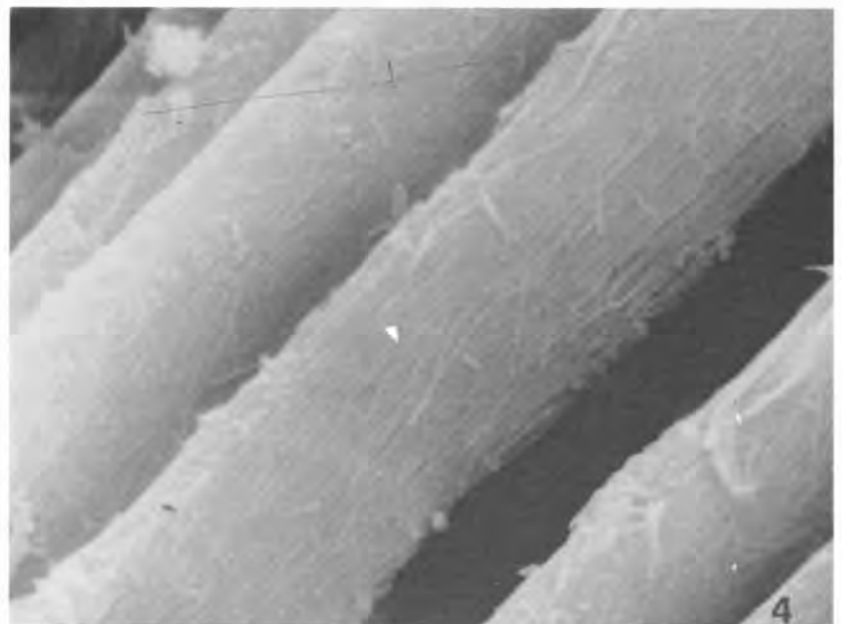


Fig. 4: 8 mm. from the cervical loop (end of the deposition zone – beginning of the maturation zone): some rod subunits are still observable. 14.200 \times .

Fig. 4: A 8 mm de l'anse cervicale (fin de la zone de dépôt – commencement de la zone de maturation): quelques sous-unités de prismes sont encore observables. 14.200 \times .

In the middle of the maturation zone, that is at 12 mm. from the cervical loop (Fig. 5), no changing in the morphology of the enamel has occurred, except for the appearance of the interrod subunits.

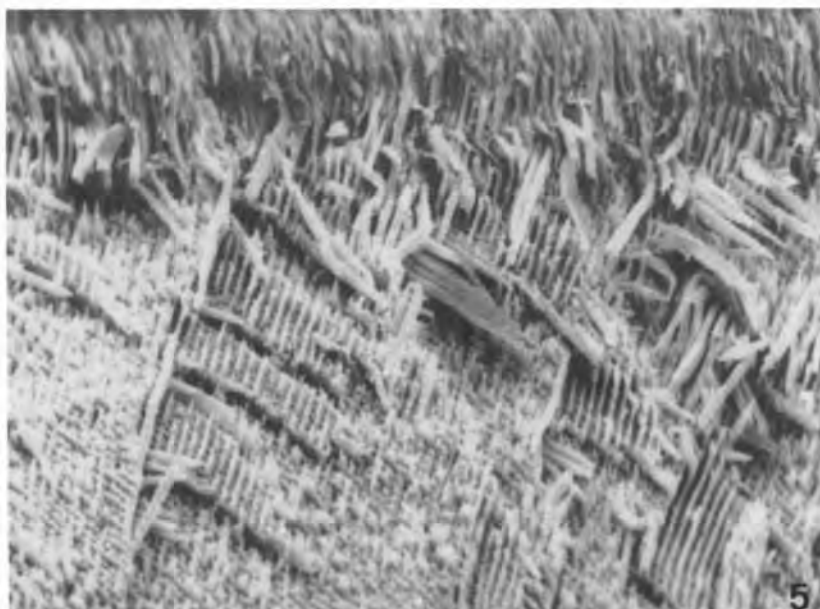


Fig. 5: 12 mm. from the cervical loop (middle of the maturation zone): appearance of the interrod subunits among the enamel rods. 700 \times .

Fig. 5: A 12 mm de l'anse cervicale (au milieu de la zone de maturation): aspect des sous-unités interprismatiques le long des prismes de l'émail. 700 \times .

Furthermore, the rods are now morphologically visible to the outer enamel layer, even if the rod subunits are still observable (Fig. 6).

Almost at the end of the maturation zone, that is at 16 mm. from the cervical loop, the interrod subunits have already accomplished their «density phase» and are characterized by enamel partitions.

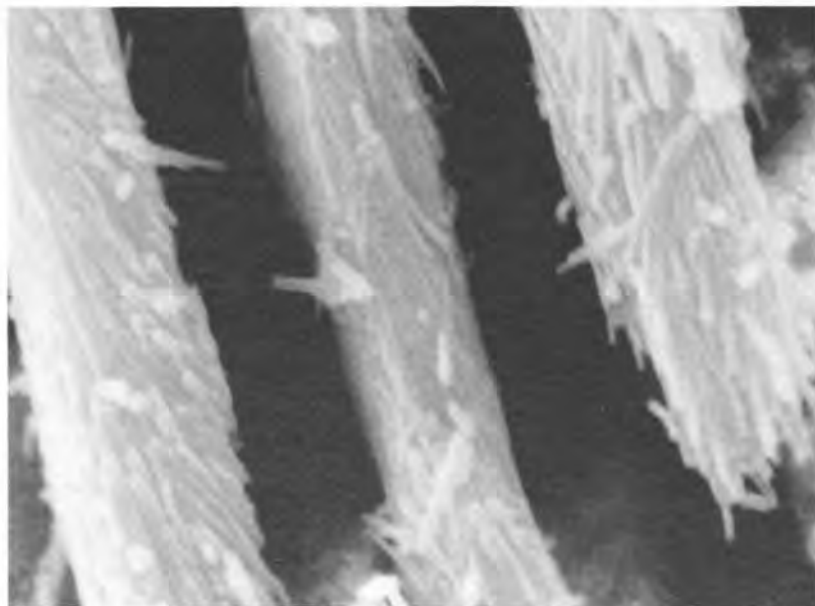


Fig. 6: 12 mm. from the cervical loop (middle of the maturation zone): some rod subunits are still observable. 12.000 \times .

Fig. 6: A 12 mm de l'anse cervicale (au milieu de la zone de maturation): certaines sous-unités de prismes sont encore observables. 12.000 \times .

These latter join the neighbouring rods together (Fig. 7). However, there are some enamel areas in which these partitions are absent (Fig 8).

In other areas both the interrod and the rod subunits are observable (Fig. 9) while in some others the enamel is in full fibrillization.

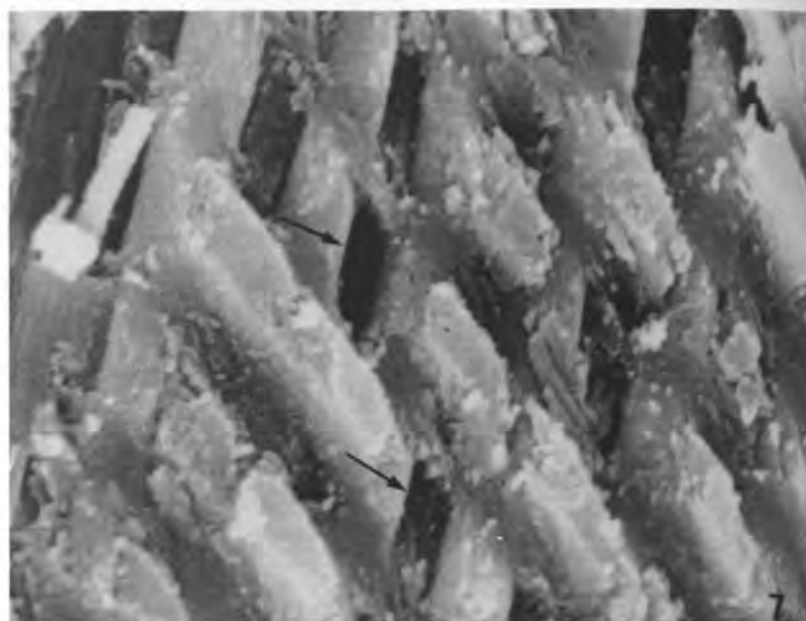


Fig. 7: 16 mm. from the cervical loop (end of the maturation zone): interrod partitions (\rightarrow) during the «density-phase». 9.000 \times .

Fig. 7: A 16 mm de l'anse cervicale (fin de la zone de maturation): séparations interprismatiques (\rightarrow) au cours de la «phase dense». 9.000 \times .

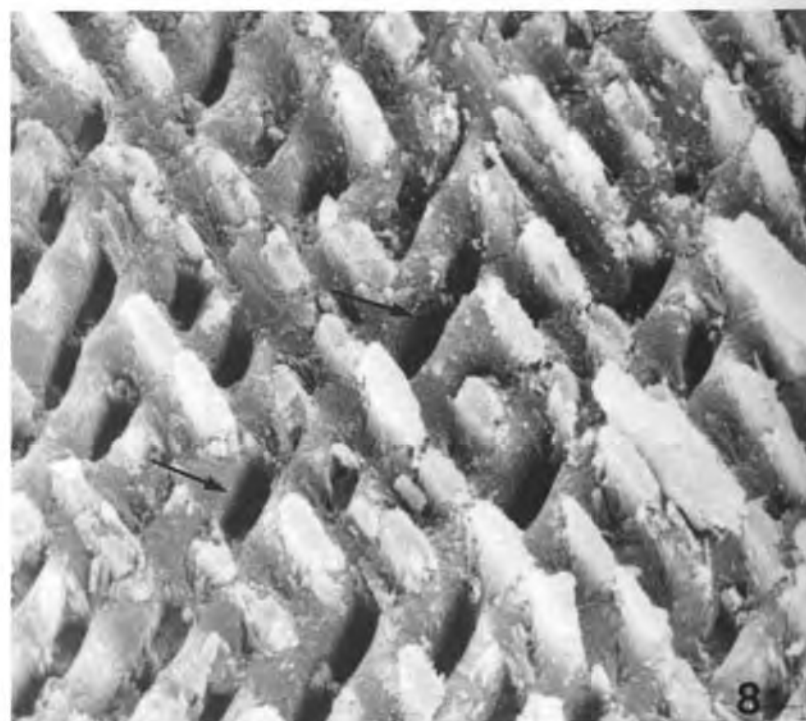


Fig. 8: 16 mm. from the cervical loop (end of the maturation zone): area in which the interrod partitions are absent (\rightarrow). 4.600 \times .

Fig. 8: A 16 mm de l'anse cervicale (fin de la maturation): région dans laquelle les séparations interprismatiques sont absentes (\rightarrow). 4.600 \times .

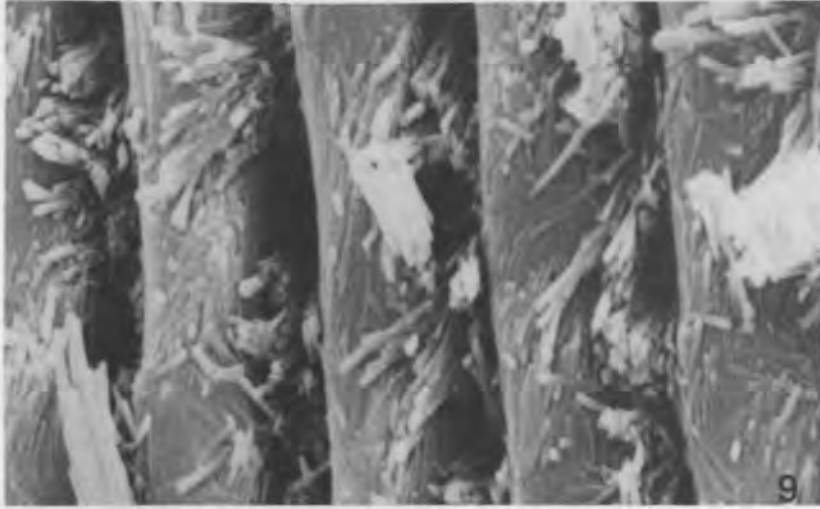
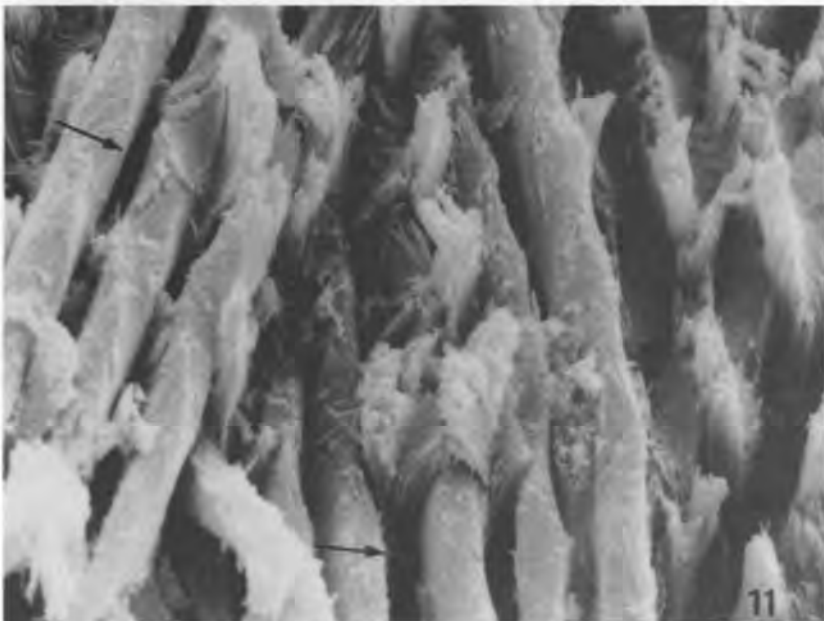
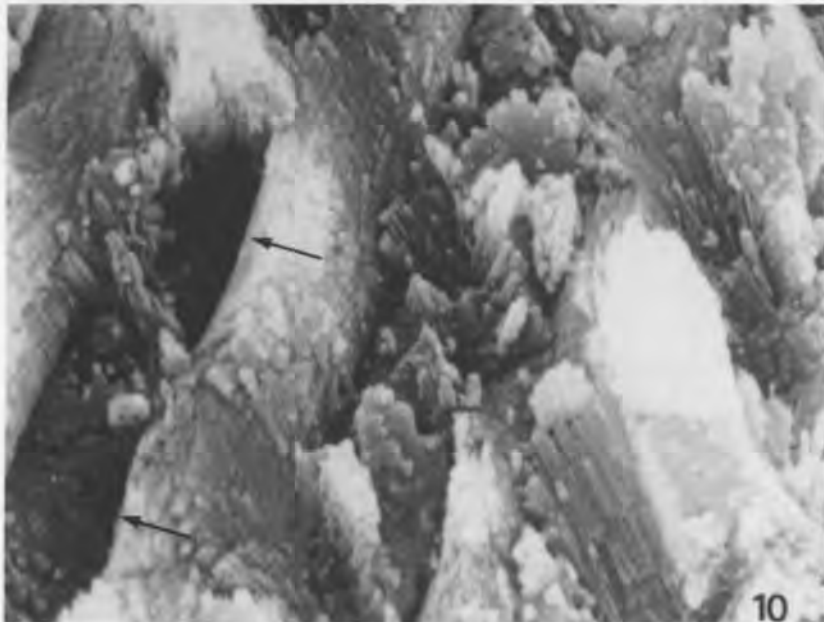


Fig. 9: 16 mm. from the cervical loop (end of the maturation zone): presence of some rod and interrod subunits. 12.600 \times .
 Fig. 9: A 16 mm de l'anse cervicale (fin de la zone de maturation): présence de quelques prismes et sous-unités de prismes. 12.600 \times .

Even at 24 mm. from the cervical loop, that is after eruption, there are some areas in which interrod partitions are absent while the full enamel fibrillization is observable (Figs. 10-11).



Ameloblasts

During the secretion phase, the ameloblasts have a very extended cylindrical shape and are joined together by desmosomes and «terminal bar» placed both at the basal and apical pole. Therefore, two different zones of secretory cells can be identified according to their ultrastructural features: the first zone corresponding to the two thirds of the secretion phase, while the second zone to the end of it.

In the first zone the nucleus is situated in the basal pole and consists of rarefied chromatin and of a clearly observable nucleolonema.

Many mitochondria are visible between the basal pole and the nucleus, while only few of them are observable between the nucleus and the apical pole. In the apical portion an ergastoplasmic reticulum, extending towards the basal portion of the Tomes' process, is evident as well as only few dense granules.

The Golgi apparatus, when present, is situated near the apical pole of the nucleus (Figs. 12-13-14).

In the second zone, as it was for the first one, the nucleus is situated near the basal pole and shows the same structural characteristics. The mitochondria are situated between the nucleus and the basal pole showing sometimes rare vacuoles (Fig. 15).

The Golgi apparatus, situated between the nucleus and the apical pole, shows rare cisterns and some vacuoles, those latter being characterized by a different density.

The cell body shows some secretion granules and many cisterns in the endoplasmatic reticulum (Fig. 16), while only rare cisterns are evident in the ergastoplasmic reticulum.

During the modulation phase the ameloblasts are shorter than before showing the nucleus in the middle of the body. The mitochondria are particularly concentrated in the apical pole (Fig. 17) and some cisterns of the ergastoplasmic reticulum, as well as some dense granules, are observable.

The apical pole is generally characterized by smooth terminal webs, only seldom by ruffle terminal webs whose invaginations, however, are not very deep (Fig. 18).

Figs. 10-11: 24 mm. from the cervical loop (erose enamel): some areas in which the interrod partitions are absent (\rightarrow). 18.300 \times ; 5.800 \times .

Fig. 10-11: A 24 mm de l'anse cervicale (émail érodé): quelques territoires dans lesquels les séparations interprismatiques sont absentes (\rightarrow). 18.300 \times ; 5.800 \times .



Fig. 12: Initial 2/3 of the secretion phase (first zone): basal portion of three ameloblasts with a nucleus characterized by rarefied chromatin and by a clearly observable nucleolonema. Presence of many mitochondria at the basal pole. 6.000 \times .

Fig. 12: Les 2/3 initiaux de la phase de sécrétion (première zone): portion basale de 3 améloblastes avec un noyau caractérisé par une chromatine raréfiée et par un nucléolonème clairement observable. Présence de nombreuses mitochondries au pôle basal. 6.000 \times .

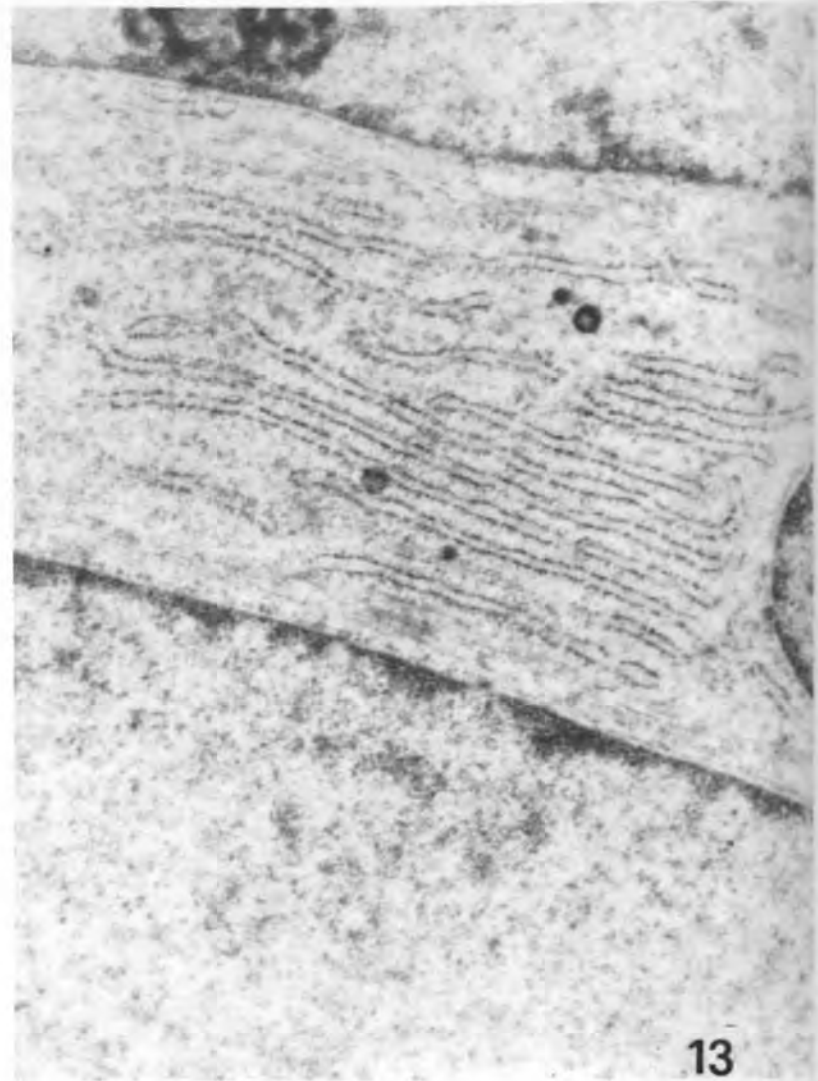


Fig. 13: Initial 2/3 of the secretion phase (first zone): a well-evident ergastoplasmic reticulum is observable in the apical portion of the ameloblast. 17.900 \times .

Fig. 13: Les 2/3 initiaux de la phase de sécrétion (première zone): un réticulum ergastoplasmique bien évident est observable dans la portion apicale de l'améloblaste. 17.900 \times .

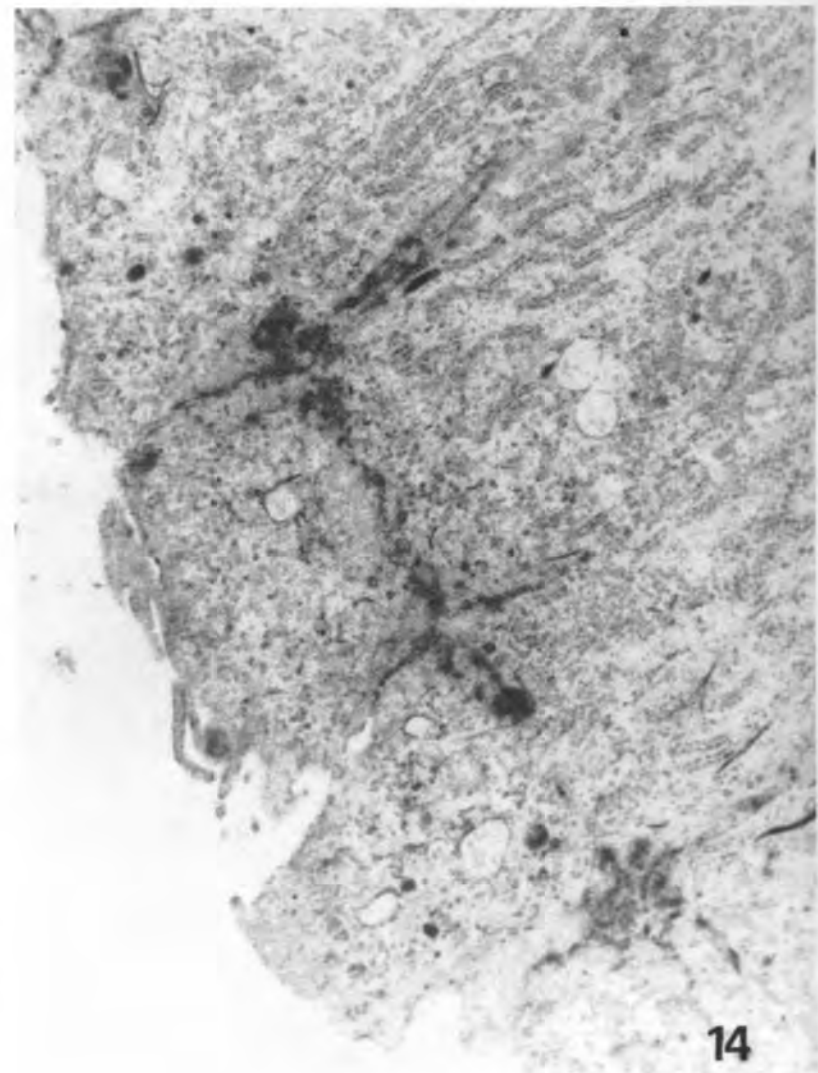
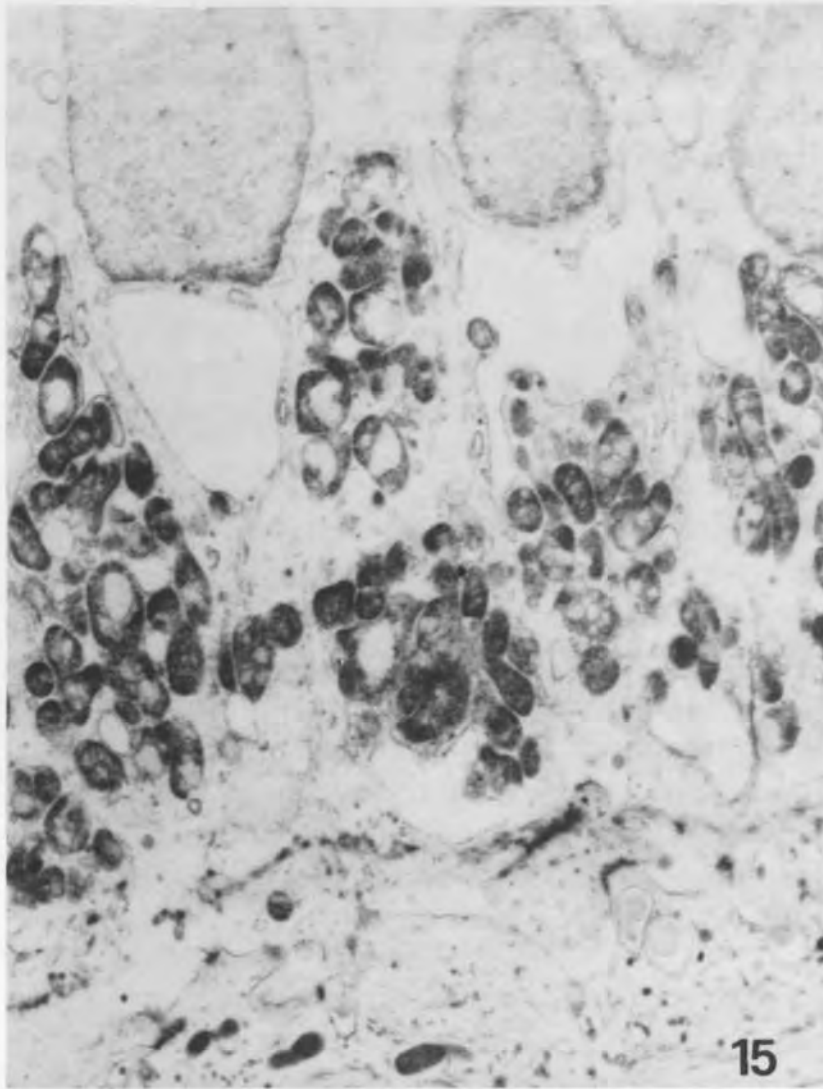
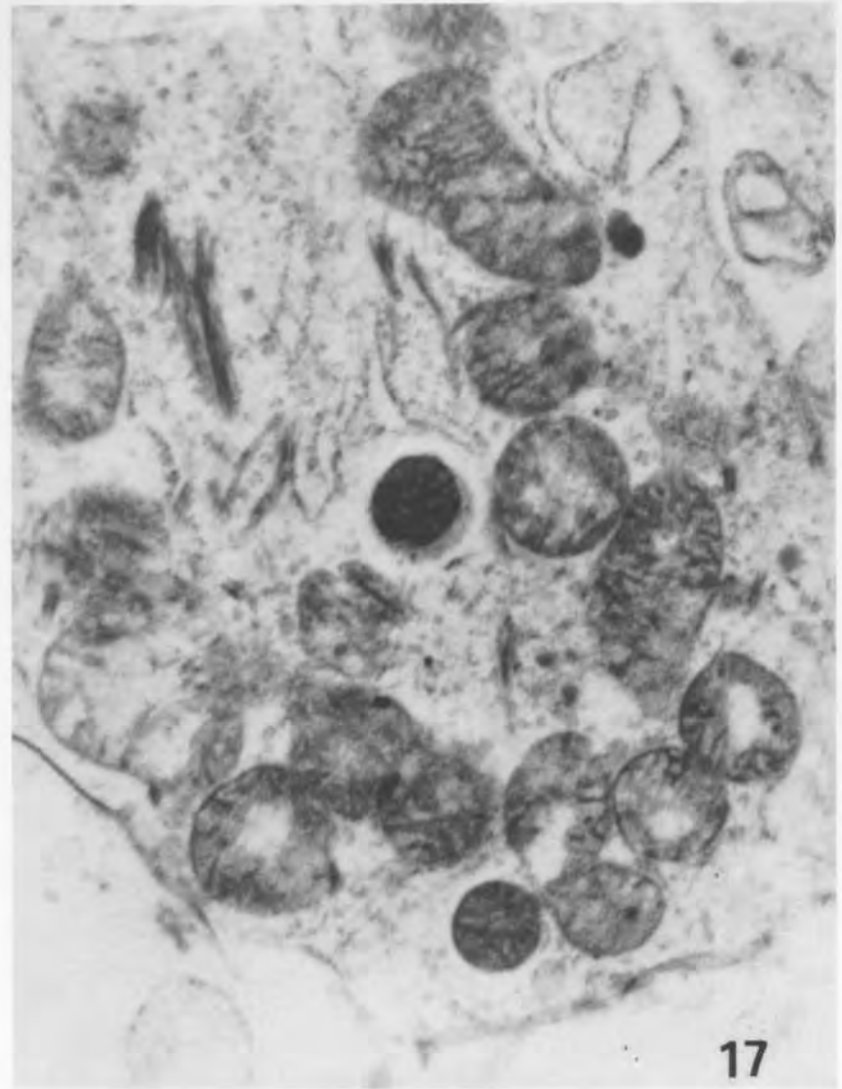


Fig. 14: Initial 2/3 of the secretion phase (first zone): two Tomes' processes, characterizing the apical pole of the secretory ameloblasts, are observable. 10.400 \times .

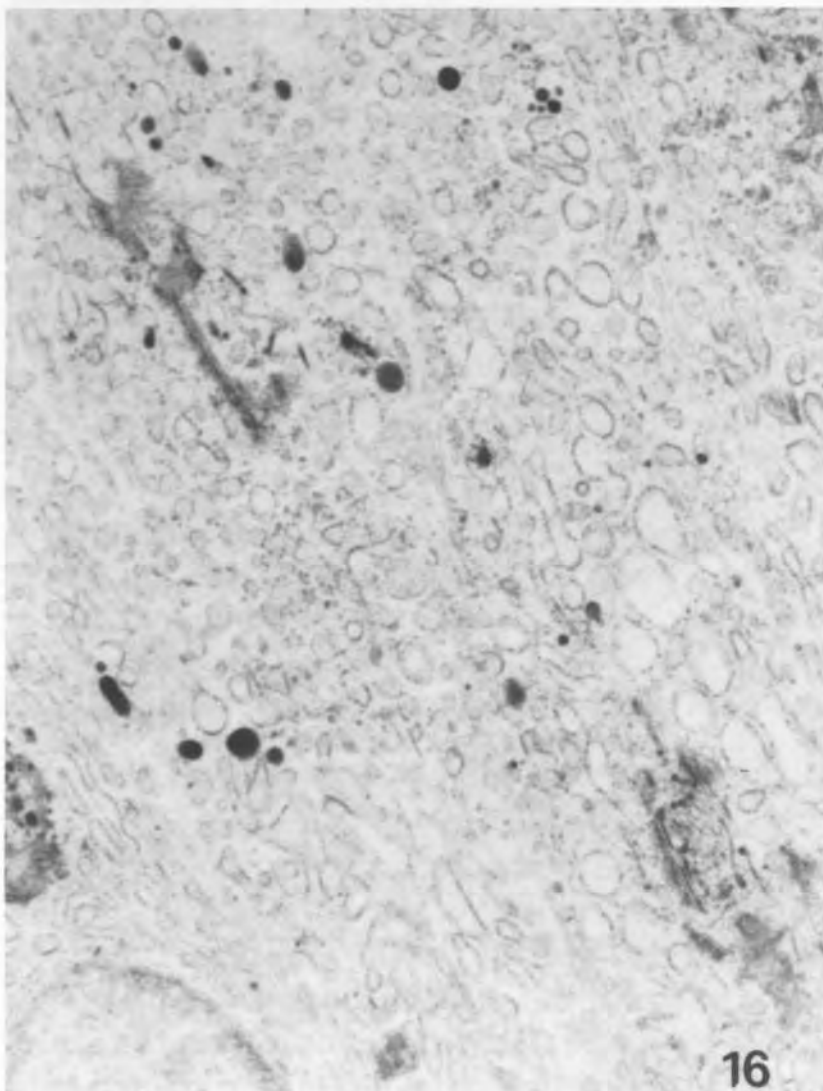
Fig. 14: Les 2/3 initiaux de la phase de sécrétion (première zone): 2 processus de Tomes caractérisant le pôle apical des améloblastes sécrétoires sont observables. 10.400 \times .



15



17



16

Fig. 15: Final 1/3 of the secretion phase (second zone): mitochondria of the basal pole showing vacuoles. 8.000 \times .

Fig. 15: Le 1/3 terminal de la phase de sécrétion (2^e zone): les mitochondries du pôle basal montrent de rares vacuoles. 8.000 \times .

Fig. 16: Final 1/3 of the secretion phase (second zone): the cell body shows some secretion granules and cisterns in the endoplasmic reticulum. 10.700 \times .

Fig. 16: Le 1/3 terminal de la phase de sécrétion (2^e zone): le corps cellulaire montre quelques grains de sécrétion et les citernes du réticulum endoplasmique. 10.700 \times .

Fig. 17: Modulation phase: in the apical pole the ameloblast shows many mitochondria. 23.800 \times .

Fig. 17: Phase de modulation: dans le pôle apical, l'améloblaste montre de nombreuses mitochondries. 23.800 \times .

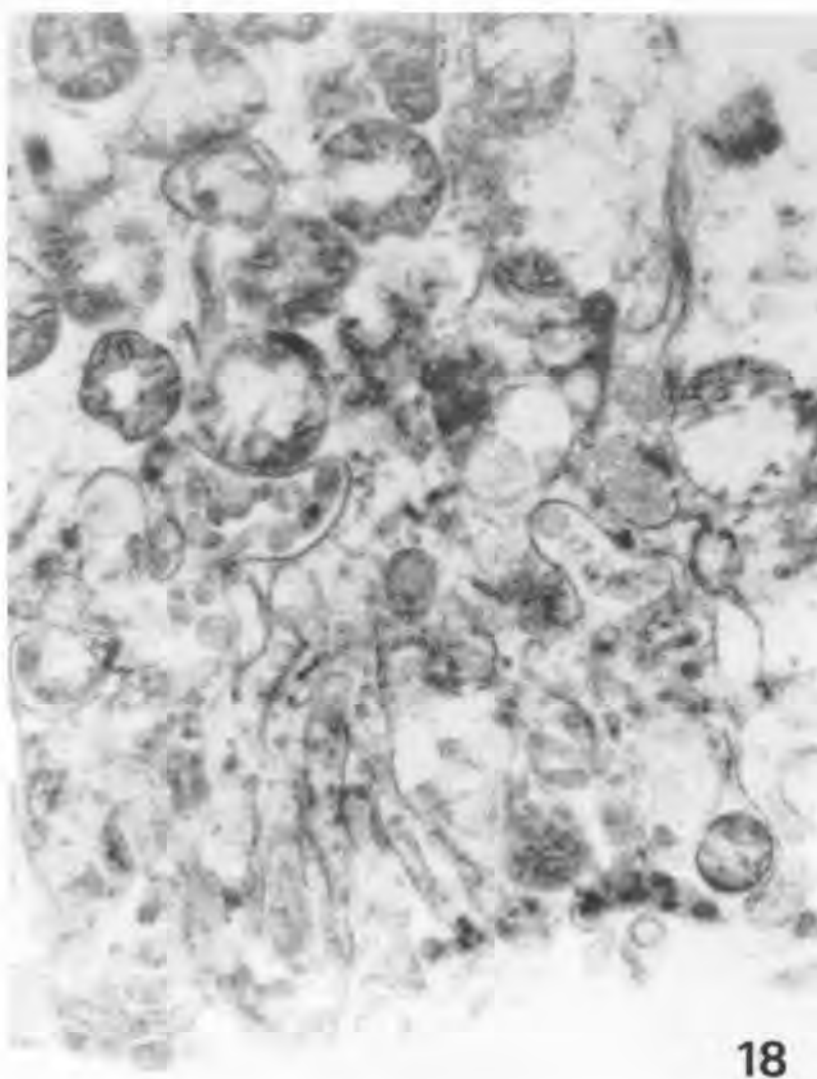


Fig. 18: Modulation phase: ruffle terminal web of the ameloblasts characterized by not very deep invaginations. 22.100 \times .

Fig. 18: Phase de modulation: l'extrémité plissée des améloblastes est caractérisée par des invaginations peu profondes. 22.100 \times .

DISCUSSION

The secretory ameloblasts are long and narrow cells showing the Tomes' process at the apical pole (Reith, 1970).

After the differentiation zone, one range of ameloblasts appears different from the following one because of the orientation of the Tomes' process distal portion.

The nucleus is situated in the basal pole and the mitochondria surround the nucleus.

A well evident ergastoplasmic reticulum is observable as well as many secretion granules.

According to what just mentioned, the administration of fluorine can be considered the principal cause for the differentiation of the two zones of secretive cells found in the present study.

At a first examination, the cells situated in the first zone show normal ultrastructural features except for the absence of mitochondria between the nucleus and the apical pole, and for the presence of rare granules.

In the second zone the cells show more evident alterations such as: mitochondrial vacuolization, a not well-defined Golgi apparatus, and an almost complete substitution of the endoplasmic reticulum for the ergastoplasmic one.

Low doses of fluorine administered to in vitro secretory ameloblasts for 8 days (Bronckers, *et al.*, 1984) caused an intracellular disorganization. On the contrary, even after 60 days of fluorine administration we found no evidence of intercellular disorganization. Therefore, even in the second zone, the ameloblasts showed their usual morphology as well as the relation between one another, this latter being possible because of the integrity of the junctional complexes.

In vitro studies have also demonstrated that fluorine administration determines a thinner enamel and the inhibition of amelogenines secretion in the ameloblasts as well as a reduced captation of Ca^{++} from the capillares of the vascular layer. The presence of reactive piroantimonium to calcium, the calcium-ATPasic activity of the cell membrane, and the numerous mitochondria in the basal pole of the cell suggest a possible mechanism of an active transport of Ca^{++} (Inage and Weinstock, 1979, Reith, 1970).

Because of the observed mitochondrial damages to the secretory ameloblasts of the second zone, we tend to believe that the reduced captation of Ca^{++} could be due to a deficit of its active transport.

Concerning the inhibition of the amelogenines synthesis, we assume that the transformation of the ergastoplasmic reticulum into the endoplasmic one, that is typical of the variation of the ameloblastic synthesis activity, supports Bronckers and coll. opinion (1984).

The enamel morphology along the transversal fracture at 4 and 8 mm. from the cervical loop, compared to the mineralization patterns proposed by Anastasi (1989), shows a slowing of the «fibrillization phase» and a very difficult start of the «density-phase», as already observed studying the incisor enamel of rats fed on hyperfluoritic pellet.

Enamel alterations can therefore be correlated with ameloblasts alterations: in fact, the amelogenines play a significant role in the nucleation of the hydroxyapatite crystals while Ca^{++} together with PO_4^{-} complexes characterize their structure.

In the present study no quantitative evaluation of enamel Ca^{++} has been carried out. Nevertheless, in previous X-ray microanalysis studies a decreased Ca^{++} and a variation of Ca/P (Magaudda, L. *et al.*, 1990) had been observed.

During the modulation phase, the cells are shorter and are also separated by larger spaces if compared to what observed during the secretion phase (Reith, 1970).

In the apical pole, a smooth terminal web always alternates with a ruffle terminal web (Josephsen and Fejerskov, 1977).

The smooth ended ameloblasts produce the lysosomal enzymes that will be then secrete, in the enamel matrix, by the ruffle ended ameloblasts in order to degrade the organic component.

This latter will be transformed into small peptides and then reabsorbed by the capillaries of the vascular layer through the intercellular spaces.

Our findings indicate that, because of the effect of fluorine the majority of the ameloblasts show a smooth terminal web.

In case of a ruffle terminal web, this is characterized by not very deep invaginations.

It has been demonstrated that the fluorine inhibits the enzymatic activity (Wiseman, 1970) and that, before eruption, the quantity of organic matrix, in the enamel treated with fluorine, is almost three times the normal one (Den Bensten and Crenshaw, 1984).

Our findings, according to the above mentioned literature, demonstrate that the decreased secretion of lysosomal enzymes, induced by fluorine during the maturation phase, reduces the organic matrix reabsorbed by the vascular layer.

Since the almost complete reabsorption of both the organic matrix and water is necessary in order that the crystallographic processes may occur (Deakins, 1942; Suga, 1982) there is no doubt that the enamel reaces the eruption not completely mineralized.

Our findings show that even after eruption, the enamel is not completely mineralized. Furthermore, our samples indicate that, both before and after erup-

tion, there are still some areas in which an incomplete aggregation of the interprismatic and intraprismatic subunits is observable.

Since the morphological pattern of the mineralization is the complete aggregation of the subunits, we can affirm that the mineralization is still incomplete.

These results correspond to those obtained in previous studies administering fluoritic pellet. A close relation between the alterations of the mineralization and the damages to the ameloblasts is therefore evident. In fact, the secretion phase is characterized by an increased cellular damage whose peculiar aspects are the mitochondrial alterations and the substitution of the endoplasmic reticulum for the ergastoplasmic one.

All this leads to an inhibition of the synthesis of the enamel proteins and to a reduction of the captation and dismission of Ca^{++} in the enamel matrix.

All these data clearly explain the slowing of the fibrillization as well as the incomplete aggregation of the rod subunits.

During the modulation phase, the cellular damages is characterized by a reduction of the number of ruffle ended ameloblasts and by a consequent reduced dismission of the lysosomal enzymes.

This determines the reduced reabsorption of the organic matrix and the incomplete aggregation of both the prismatic and the interprismatic subunits.

CONCLUSIONS

Our findings have shown that it is possible to obtain equal alterations of the mineralization process administering fluorine either using fluoritic water of fluoritic pellets.

In particular, we observed the slowing of the fibrillization as well the slowing of the density phase, of both the rod and the interrod, leading to the presence of some hypomineralized areas after eruption.

Furthermore, the alterations of the ameloblasts, e.g. the mitochondrial damage, the presence of a well-evident endoplasmic reticulum, the lack in dense granules during the secretion phase and the rare ruffle ended webs during the modulation phase, justify the slowing of the enamel mineralization due to the fluorine effect on the ameloblasts.

REFERENCES

- [1] Anastasi, G. — Mineralizzazione e struttura dello smalto (Studio al M.E.S. ed alla microanalisi a rX nell'incisivo inferiore di ratto albino). *Arch. Ital. Anat. Embriol.*, 94, 2: 97-152, 1989.
- [2] Anastasi, G., Bruschetta, D., De Leo, S., Magaudo, L., Santoro, G., Trimarchi, F. — Mineralizzazione dello smalto in ratti sottoposti a dieta iperfluorica: studio al M.E.S. *Minerva Stomatologica*, 39, 9: 705-714, 1990.
- [3] Bronkers, A.L.J.J., Jansen, L.L., Wolgens, J.H.M. — A histological study of the short term effects of fluoride on enamel and dentine formation during hamster tooth germ development in organ culture. *Arch. Oral. Biol.*, 29: 803-810, 1984.
- [4] Deakins, M. — Changes in the ash, water and organic contents of pig enamel during calcification. *J. Dent. Res.*, 21: 429-435, 1942.
- [5] Den Best, P.K., Creenshaw, M.A. — The effect of chronic high fluoride levels on forming enamel in the rat. *Arch. Oral. Biol.*, 29: 675-679, 1984.
- [6] Eanes, D. — Enamel apatite: Chemistry, structure and properties. *J. Dent. Res.*, 58(B): 829-834, 1979.
- [7] Josephesen, K., Fejerskov, O. — Ameloblast modulation in the maturation zone of the rat incisor enamel organ. A light and electron microscopic study. *J. Anat.*, 124-145, 1977.
- [8] Kruger, B.J. — Interaction of fluoride and molibdenum on dental morphology in the rat. *J. Dent. Res.*, 45: 714-725, 1966.
- [9] Inage, T., Weinstock, A. — Localization of enzyme ATP-ase in the rat secretory ameloblasts by means of electron microscopy. *J. Dent. Res.*, 58(B): 1010-1011, 1979.
- [10] La Spada, E., Busà, S. — Rilievi clinico-statistici sulla fluorosi endemica e sulla carie dentale in alcune zone della Calabria. *Giorn. Odontostomatol.*, 4: 1-8, 1968.
- [11] Leverett, D.H., Jensen, O.E. — Dental caries and staining after twenty-eight months of rinsing with stannous fluoride or sodium fluoride. *J. Dent. Res.*, 65: 424-427, 1986.
- [12] Magaudo, L., Santoro, G., Pisani, G., Pino, G., Vaccaro, M. — Ricerche in microanalisi a Rx sullo smalto in via di mineralizzazione in ratti sottoposti a dieta iperclorica o iperfluorica. XLIV Congresso Nazionale della Società di Anatomia, Bologna 24-26 Settembre 1990.
- [13] Reith, E.J. — The stages of amelogenesis as observed in molar teeth of young rats. *J. Ultrastr. Res.*, 30: 111, 1970.
- [14] Reynolds, E.S. — The use of lead citrate at pH as an electron opaque stain in electron microscopy. *J. Cell. Biol.*, 17: 208-212, 1963.
- [15] Sortino, G., Munaò, R., Calabrò, R., Briguglio, E. — Endemia di fluorosi dentale ed alta percentuale di carie in una zona della Calabria. *Arch. ed. Atti della Soc. Med. Chir. di Messina*, XII (Fasc. III): 1-7, 1968.
- [16] Suga, S. — Progressive mineralization pattern of developing in enamel during the maturation stage. *J. Dent. Res.*, 61: 1532-1542, 1982.
- [17] Wiseman, A. — Effect of inorganic fluoride on enzymes. In: Smith, F.A., ed. *Pharmacology of Fluoride*, Part II. Berlin: Springer Verlag, 2, 48-97, 1970.

Correspondence address:
S. Pergolizzi,
Department of Biomorphology,
Via P. Castelli, 40 - 98122 Messina (Italy).